SOLAR PHYSICS SIMULATIONS WITH THE VERSATILE ADVECTION CODE

Gábor Tóth

Eötvös University, Pázmány P. sétány 1/A, H-1117 Budapest, Hungary
tel.: +36-1-3722750, fax: +36-1-3722753, e-mail: gtoth@hermes.elte.hu

ABSTRACT

The Versatile Advection Code is a general purpose hydrodynamic and magnetohydrodynamic software package. It uses modern shock capturing schemes with explicit or implicit time stepping on one, two, or three dimensional finite volume grids. Initial and boundary conditions and different source terms can be defined by parameters and/or user written subroutines. The Versatile Advection Code can be compiled with a Fortran 77, Fortran 90, or High Performance Fortran compiler and it runs efficiently on platforms ranging from personal computers and work stations to vector and parallel supercomputers. The code can be obtained via registration from `http://www.phys.uu.nl/~toth`.

In this paper, I demonstrate the capabilities of the Versatile Advection Code by showing five different solar physics applications which have already resulted in publications.

Key words: MHD; Methods: numerical

1. INTRODUCTION

The aim of developing the Versatile Advection Code (VAC, Tóth 1996; Tóth 1997b) is to provide the astrophysicist and physicist community with a modern, versatile, and user-friendly software, which can be adapted to the application. VAC can solve the hydrodynamic and adiabatic hydrodynamic equations, the isothermal or polytropic MHD equations, and the full MHD equations. Source terms for diffusion, resistivity, viscosity, heat conduction, radiative cooling, and external and self-gravity are readily available, other types of source terms can be defined in user written subroutines.

VAC uses various shock capturing numerical methods: two versions of Flux Corrected Transport (FCT, Boris & Book 1973; Odstrčil 1993) schemes, the Lax-Wendroff type Total Variation Diminishing (TVD, Harten 1983) and the TVD-MUSCL (van Leer 1979) schemes with Roe-type approximate Riemann solvers (Roe 1981; Roe & Balsara 1996), and the TVD-Lax Friedrichs (TVDLF, Yee 1989) method. For exact specifications of these algorithms, see Tóth & Odstrčil (1996). Explicit, semi-implicit, or fully implicit time stepping (Keppens et al. 1999; Tóth et al. 1998) algorithms are available for time integration. The simulations can be done on 1, 2, or 3 dimensional structured finite volume grids using the same dimensional independent source code written in the Loop Annotation Syntax (Tóth 1997a). In two spatial dimensions both slab and cylindrical symmetry can be assumed in the ignored third dimension. Cartesian and polar grids are handled as special cases for sake of efficiency. For multidimensional MHD applications, the divergence of the magnetic field can be kept zero with the projection scheme (Brackbill & Barnes 1980), or with the constrained transport/central difference (Evans & Hawley 1988; Tóth 1999) approach. Also implemented in VAC are Powell's eight-wave Riemann solver and the corresponding source terms (Powell 1994; Gombosi et al. 1994).

VAC runs efficiently on personal computers, work stations, and vector and parallel super computers as well. On scalar and vector machines, any Fortran 77 or Fortran 90 compiler can be used. Parallel execution of the code is achieved by an automatic translation to High Performance Fortran. All explicit schemes, including the projection scheme, are fully parallelizable.

The software package is complete with manual pages written in hypertext, a user interface based on web browsers, data conversion programs for different platforms and for different softwares (e.g. AVS, DX and Gnuplot) and visualization macros for the most popular visualization softwares, IDL, Matlab, and SM. In fact, most of the figures presented in this paper were produced with the IDL macros provided with VAC. The user friendly environment has already helped more than 30 scientists in their research. See `http://hermes.elte.hu/~gtoth/Papers/vac.html` for an ever growing list of publications.

In the following section, I will illustrate the versatility of the code on five solar physics problems, which have already led to publications.

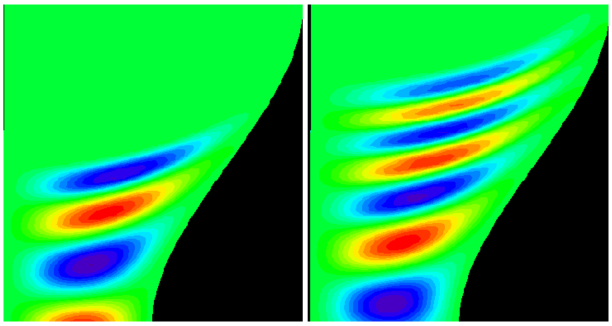

Figure 1. Two snapshots of the B_φ component of a running Alfvén wave in a coronal hole which is 'flaring-out' in the radial direction

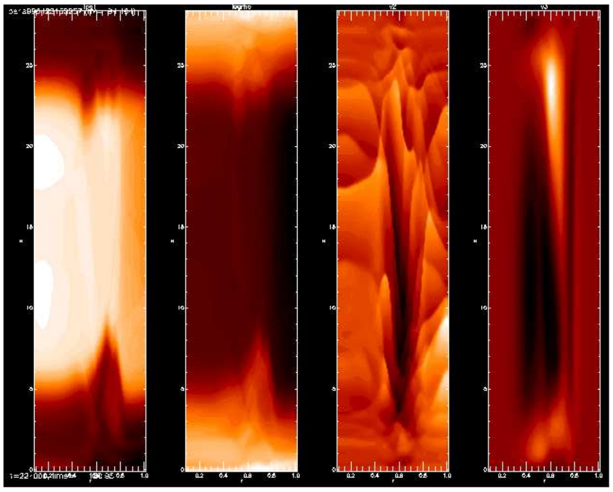

Figure 2. Snapshot of the spatial dependence of $\log T$, $\log\rho$, v_z, *and* v_θ *in a closed loop. Horizontally the radial and vertically the longitudinal dependence is plotted. The minimum/maximum values of* v_z *and* v_θ *are* ± 40 *km/s and* ± 100 *km/s respectively. In all frames, white represents maximum and black minimum values.*

2. APPLICATIONS

For each application, first the physical problem and the results are described, following closely the abstracts of the published papers. Next, I discuss the equations, the source terms, the geometry, and the corresponding discretization. I will point out the numerical difficulties and give hints, how these were avoided by a good choice of discretization and/or numerical scheme.

2.1. Nonlinear MHD Simulations of Wave Dissipation in Flux Tubes

Poedts et al. (1997) studied Alfvén wave propagation and phase mixing in open flux tubes flaring out in the corona. The resulting energy transfer from large to small length scales contributes to the heating of these magnetic structures. In coronal holes, the *phase-mixing* of running Alfvén waves is *speeded-up* by the 'flaring-out' of the magnetic field lines in the lower chromosphere.

The open loop problem is studied by VAC solving the MHD equations on a 2.5D structured grid assuming axial-symmetry in the 3rd dimension. The structured grid follows the shape of the magnetic field lines, thus the affects of flaring on wave propagation can be modeled without the complexity of simulating the surrounding corona, which should maintain the pressure equilibrium and provide stability. The initial condition and the grid for a flaring loop was produced by a finite element code, PARIS (by S. Beliën). Alfvén waves were induced by shaking the field lines at the chromosphere and their propagation into the corona is calculated with the dimensionally unsplit TVD-MUSCL scheme in VAC.

2.2. Coronal Heating by Resonant Absorption: the Effects of Chromospheric Coupling

Beliën et al. (1999) examined resonant absorption of Alfvén waves in closed loops penetrating through the transition region. They present the first 2.5D numerical model calculations of the nonlinear wave dynamics and heating by resonant absorption in coronal loops with thermal structuring of the transition region and higher chromosphere. The transition region can move freely and is transparent for mass motions from chromosphere to corona. The loops are excited at the chromospheric level by linearly polarized monochromatic Alfvén waves. They find that the efficiency of resonant absorption can be much lower than in equivalent line-tied coronal loop models. While the efficiency of resonant absorption heating is low, the results indicate that heating by compression and dissipation of the slow magnetosonic waves and shocks can easily lead to a temperature rise of a few percent and for larger driver amplitudes even to a rise over ten percent. Hence, the results support the idea for indirect coronal heating through the nonlinear generation of magnetosonic waves that has been put forward more than twenty years ago. Furthermore, the large transition region and coronal density oscillations that are associated with the slow magnetosonic waves provide an explanation for some observed coronal and transition region loop EUV intensity variations. *See the proceedings of Beliën et al. for more details.*

The full system of MHD equations is solved with external gravity, radiative cooling, and thermal conduction parallel to the magnetic field. The closed loop is straightened into a cylinder, i.e. curvature effects are neglected. Assuming axial symmetry, the problem can be modeled in 2.5D on a Cartesian grid. At both ends of the cylinder, the chromosphere is modeled as a high density, low temperature plasma. The loop is driven with Alfvén waves at one of the ends. The Lax-Wendroff type TVD scheme is used in a dimensionally split fashion, which handles the contact discontinuity in the transition region with minimal diffusion. The numerical results were confirmed with the FCT scheme.

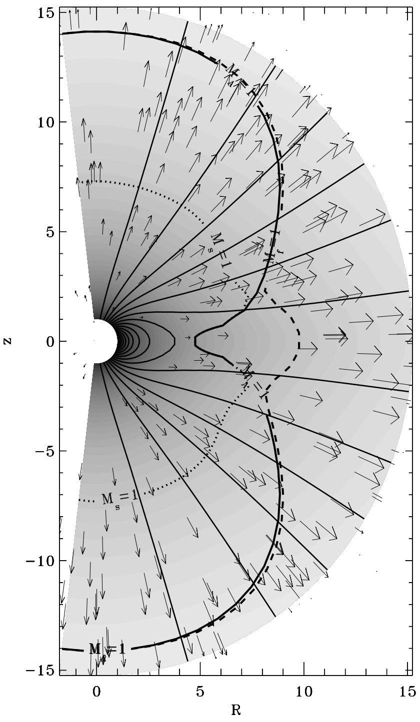

Figure 3. Axisymmetric wind solution containing a 'dead' zone. Shown are the poloidal magnetic field lines, and the poloidal velocity (vectors). The three critical surfaces are indicated.

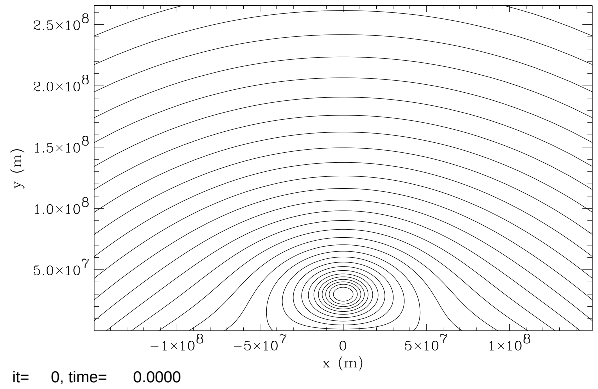

Figure 4. The magnetic field topology. A strong, localized current runs near $(x, y) = (0, 3 \times 10^7)$ m, at the location of the prominence. Only the central part of the full computational domain is shown, which has dimensions $3 \times 10^9 \times 1.5 \times 10^9$.

2.3. Numerical Simulations of Stellar Winds: polytropic models.

Keppens & Goedbloed (1999a,1999b) obtained steady state solutions for different models of the solar wind in one and two dimensions. They discuss steady-state transonic outflows obtained by direct numerical solution of the hydrodynamic and magnetohydrodynamic equations. They proceed stepwise from a spherically symmetric, isothermal, unmagnetized, non-rotating Parker wind to arrive at axisymmetric, polytropic, magnetized, rotating models. These represent 2D generalisations of the analytical 1D Weber-Davis wind solution: thermally and/or magneto-centrifugally driven stellar outflows can be modeled. Axisymmetric wind solutions containing both a 'wind' and a 'dead' zone are also presented.

The 1D problems are solved in spherical symmetry both for the adaiabatic hydrodynamic and the polytropic MHD equations. This way, there is no need to model the poorly understood heating and cooling processes of the corona. The only source term is the external gravitation due to the star. For the 2D solution, a generalized grid is used in the poloidal plane (following the $r - \theta$ coordinates) and axial symmetry is assumed in the azimuthal φ direction. The steep gradients close to the solar surface are resolved by a logarithmic grid accumulation. Since steady-state solutions are sought, a fully implicit time stepping is used. The initial condition is obtained from the corresponding one-dimensional solution. For the spatial discretization, the very robust dimensionally unsplit TVDLF scheme was chosen. The boundary conditions imposed at the stellar surface are very important, they have to ensure that the velocity and the magnetic fields are parallel in the frame corotating with the star.

This work has been continued towards time dependent and 3D models. *See the proceedings of Keppens and Goedbloed for details.*

2.4. Numerical Simulations of Prominence Oscillations

Schutgens & Tóth (1999) modeled oscillations of an inverse polarity prominence. The internal prominence equilibrium, the surrounding corona and the inert photosphere are well represented. Gravity and thermodynamics are not taken into account, but it is argued that these are not crucial. The oscillations can be understood in terms of a solid body moving through a plasma. The mass of this solid body is determined by the magnetic field topology, not by the prominence mass proper. The model also allows us to study the effect of the ambient coronal plasma on the motion of the prominence body. Horizontal oscillations are damped through the emission of sound waves while vertical oscillations are damped through the emission of Alfvén waves.

The isothermal MHD equations are solved on a 2.5D non-uniform Cartesian grid with the FCT algorithm, which is quite accurate for smooth problems. Since no analytical equilibrium solution is known, the initial conditions for the arcade and the prominence are obtained by a sophisticated relaxation procedure. Then the stationary prominence is kicked, and the the resulting damped oscillations are calculated by the code. The non-reflecting coronal boundary conditions are achieved by the strongly stretched grid, which places the boundaries far away. This is important to minimize boundary effects on the damping rate. The photosphere is modeled as a solid wall with field lines frozen in at an angle.

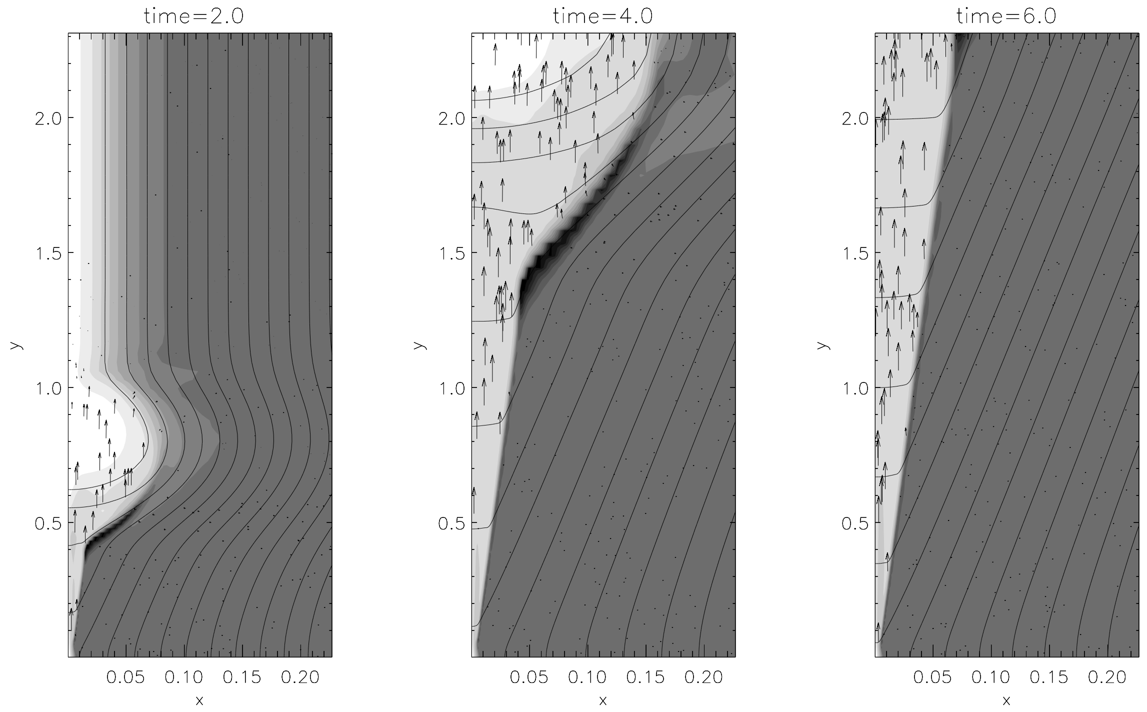

Figure 5. Evolution of uniform density current sheet. Shown are the temperature (dark tones correspond to high temperature), velocity vectors, and magnetic field lines. Only a small part of the full computational domain is plotted and the x direction is strongly stretched.

2.5. Simulations of Small-Scale Explosive Events on the Sun

Innes & Tóth (1998) studied the time evolution of Petschek type reconnection as a possible model for small-scale explosive events or microflares, which occur throughout the chromospheric network of the Sun. They are seen as sudden bursts of highly Doppler shifted spectral lines of ions formed at temperatures in the range $2 \times 10^4 - 5 \times 10^5$ K. They tend to occur near regions of canceling photospheric magnetic fields and are thought to be directly associated with magnetic field reconnection. Recent observations have revealed that they have a bi-directional jet structure reminiscent of Petschek reconnection. We do compressible MHD simulations of the evolution of a current sheet to a steady Petschek, jet-like configuration. We obtain velocity profiles that can be compared with recent ultraviolet line profile observations. By choosing initial conditions representative of magnetic loops in the solar corona and chromosphere, it is possible to explain the fact that at Sun center the jet flowing outward into the corona is more extended and seen before the jet flowing towards the chromosphere. Although this model can reproduce the high Doppler shifted components of the line profiles, the brightenings at low velocities, near the center of the bi-directional jet, cannot be explained by this simple MHD model.

The resistive MHD equations are solved on a 2D non-uniform Cartesian grid with the TVDLF method. Radiative cooling source terms are used in the energy equation. The initial conditions are relatively simple: a current sheet in pressure equilibrium. Due to the mirror symmetries, Only one quater of the physical problem is modelled, thus the boundary conditions are symmetric at the x and y axes. To minimize boundary affects, the other boundaries are non-reflective, and they are placed far from the currect sheet using a stretched grid. Reconnection of antiparallel field lines is induced by a localized anomalous resistivity at $x = y = 0$. The time evolution of the jet formation (see Fig. 5 can be best followed by explicit time integration, while the final steady state can be more efficiently calculated with a fully implicit scheme. Line profiles of the emission coming from the explosive event are calculated from the simulation data saved by VAC.

The proceedings by Roussev, Erdélyi, Doyle, and Galsgaard shows similar simulations obtained with a different code.

3. CONCLUSIONS

This paper has presented several solar physics problems where the Versatile Advection Code has been used for numerical simulations. My intention was to give an impression of the physical problems, the obtained results, and the numerical techniques for each application. It is my hope that these examples will motivate solar physicists in identifying new problems where the Versatile Advection Code may help their research.

ACKNOWLEDGEMENTS

I thank the first authors S. Beliën, D. Innes, R. Keppens, N. Schutgens, and S. Poedts for their permission on using the abstracts and some representative figures of the respective papers. The Versatile Advection Code has been developed as part of the project on 'Parallel Computational Magneto-Fluid Dynamics', funded by the Dutch Science Foundation (NWO) from 1994 to 1997. My current research is supported by the Hungarian Science Fundation (OTKA, grant D 25519) and the Bolyai Fellowship of the Hungarian Academy of Sciences. Last but not least, I am very grateful to the Local Organizing Committee, whose financial support helped me in attending this conference.

REFERENCES

A. J. C. Beliën, P. C. H. Martens, R. Keppens 1999, Coronal heating by resonant absorption: the effects of chromospheric coupling, accepted by ApJ

J. P. Boris, D. L. Book 1973, J. Comput. Phys., 11, 38

J. U. Brackbill, D. C. Barnes 1980, J. Comput. Phys., 35, 426

C. R. Evans, J. F. Hawley 1988, ApJ, 332, 659

T. I. Gombosi, K. G. Powell, D. L. De Zeeuw 1994, J. Geophys. Res., 99, 21,525

A. Harten 1983, J. Comput. Phys., 49, 357

D. E. Innes, G. Tóth 1998, Solar Phys., 185, 127

R. Keppens, J. P. Goedbloed 1999a, A&A, 343, 251

R. Keppens, J. P. Goedbloed 1999b, in proceedings of SOHO 7 Workshop (Northeast Harbor, Maine, USA) on Coronal Holes and Solar Wind Acceleration, Space Sci. Rev., 87, 223

R. Keppens, G. Tóth, M. A. Botchev, A. van der Ploeg 1999, Int. J. for Num. Meth. in Fluids, 30, 335

D. Odstrčil 1993, J. Comput. Phys., 108, 218

S. Poedts, G. Tóth, A. J. C. Beliën,, J. P. Goedbloed 1997, Solar Phys., 172, 45

K. G. Powell 1994, ICASE Report No 94-24, Langley, VA

P. L. Roe 1981, J. Comput. Phys., 43, 357

P. L. Roe, D. S. Balsara 1996, SIAM J. Appl. Math., 56, 57

N. A. J. Schutgens, G. Tóth 1999, A&A, 345, 1038

G. Tóth 1997b, J. Comput. Phys., 138, 981

G. Tóth 1997a, Lecture Notes in Comp. Sci., 1225, 253

G. Tóth 1996, Astrophys. Lett. & Comm., 34, 245

G. Tóth 1999, The $\nabla\cdot\mathbf{B}=\mathbf{0}$ Constraint in Numerical Magnetohydrodynamics, J. Comput. Phys., submitted

G. Tóth, R. Keppens, M. A. Botchev 1998, A&A, 332, 1159

G. Tóth, D. Odstrčil 1996, J. Comput. Phys., 128, 82

B. van Leer 1979, J. Comput. Phys., 32, 101

H. C. Yee 1989, NASA TM-101088